Continuous and Discrete Adjoints to the Euler Equations for Fluids *

Frédéric Alauzet[†]   Olivier Pironneau [‡]

January 19, 2013

Abstract

Adjoints are used in optimization to speed-up computations, simplify optimality conditions or compute sensitivities. Because time is reversed in adjoint equations with first order time derivatives, boundary conditions and transmission conditions through shocks can be difficult to understand. In this article we analyze the adjoint equations that arise in the context of compressible flows governed by the Euler equations of fluid dynamics. We show that the continuous adjoints and the discrete adjoints computed by automatic differentiation agree numerically; in particular the adjoint is found to be continuous at the shocks and usually discontinuous at contact discontinuities by both.

Introduction

In optimization adjoints greatly speed-up computations; the technique has been used extensively in CFD for optimal control problems and shape optimization (see [14, 20, 22, 17, 11] and their bibliographies). Because time is reversed in adjoint equations and because convection terms operate in the opposite direction, boundary conditions and transmission conditions through shocks can be difficult to understand. Automatic differentiation in reverse mode [10],[13] automatically generates the adjoint equations so the problem does not arise because boundary conditions are set by the adjoint generator. But the problem then is to understand and make sure that there is a limit when the mesh size tends to zero and that this limit agrees with the continuous solution.

Answering these questions is important for design of supersonic airplanes because shocks are involved; a good case study is the design of airplanes with the least sonic boom at ground level. Several investigations have been done already (see B. Mohammadi et al [20], S. Kim et al [15], A. Loseille et al [19], M. Nemec [21] and the bibliography therein) and automatic differentiation is

---

known to work also in this case. Another application is the optimization of "goal oriented meshes" [3] which minimize the numerical error to compute a functional like drag or lift [19].

Finite volume schemes for the Euler equations work also for the linearized Euler equations, and so should work equally well on the differentiated Euler system. However the variables of the differentiated Euler equations are much less regular than those those of the Euler equations: being derivatives of discontinuous functions the sensitivities of the flow variables have Dirac singularities and it is not at all clear that a finite volume method is capable of computing such solutions; thus the discrete adjoint systems derived by automatic differentiation in reverse mode are based on dubious assumptions. In other words we may have a convergence problem: does the discrete adjoint state converge to some continuous state? Is it solution of a continuous adjoint equations; and since there may not be a unique way to set up an adjoint for a given optimization problem (see Giles[7]), which adjoint is it?

All these questions have been addressed in the case of scalar conservation laws in one dimension of space by Ulbrich et al. [27, 9]. A framework was also introduced in [27] and [2] which can be extended to multidimensional vector systems of conservation laws but the theory of course is lacking. So we propose here to recall the formalism and do detailed numerical tests to check if the results obtained in one dimension of space extends to two and three dimensions. Our answers are encouraging: discrete and continuous extended calculus of variations agree; the discrete adjoints seem to converge to the continuous ones; when the mesh is refined the method is stable and gives better solutions.

1 Preliminaries

1.1 Calculus of Variations

Consider the following problem

$$\min_a \{ J(u, a) \ : \ L(u) = f(a) \} \tag{1}$$

where $u \to L(u)$ is an unbounded operator, like a partial differential system, from a Hilbert space U to another Hilbert space V.

When a varies, everything varies up to higher order terms according to

$$\delta J = J'_u \delta u + J'_a \delta a, \ \text{with} \ L'(u) \, \delta u = f'_a \delta a. \tag{2}$$

For Problem (1), the adjoint state is $u^* \in V^*$, the solution of $L^* u^* = J'_u$, i.e.

$$< L^* u^*, v > := < u^*, L'(u)v > = J'(u)v, \ \forall v \in U \tag{3}$$

where $< \cdot, \cdot >$ denotes the duality product between the spaces and their duals, U and U^* in the first instance and V and V^* in the second.

From these definitions we can derive another expression for δJ because

$$J'_u \delta u = < L^* u^*, \delta u > = < u^*, L' \, \delta u > = < u^*, f'_a \delta a > \tag{4}$$

and finally

$$\delta J = < f'^*_a u^* + J'_a, \delta a > . \tag{5}$$

This is a very useful result because it implies that at the solution we have: $f'^*_a u^* + J'_a = 0$, the so-called optimality conditions. It also says that an iterative scheme like

$$a^{m+1} = a^m - \lambda (f'^*_a u^* + J'_a)^*|_{a=a^m} \tag{6}$$

is a steepest descent algorithm which will converges for a small enough step size $\lambda \in \mathbf{R}^+$.

This calculus is formal but can be justified under continuity and differentiability hypotheses of all functions and operators; the difficulty is to show that the higher order terms are indeed small.

2 An example with the Euler equations for incompressible flows

2.1 The Continuous Case

Consider an optimization problem for an incompressible inviscid Euler flow. The velocity of the fluid is denoted u the pressure p, the domain occupied by the fluid Ω; it could be the 2D cross section of a nozzle with an inflow boundary Γ^-, an outflow boundary Γ^+ and walls Γ^0. One seeks for a nozzle inflow velocity a leading to a velocity u_d in a region of space $D \subset \Omega$:

$$\min_a \{ J(u) = \frac{1}{2} \int_{D \times (0,T)} |u - u_d|^2 \; : \partial_t u + \nabla \cdot (u \otimes u) + \nabla p = 0, \; \nabla \cdot u = 0,$$
$$u_{t=0} = 0, \; u|_{\Gamma^-} = a, \; u \cdot n|_{\Gamma^+} = b, \; u \cdot n|_{\Gamma^0} = 0 \} \tag{7}$$

where n is the outer normal to $\Gamma := \partial \Omega = \Gamma^- \cup \Gamma^+ \cup \Gamma^0$. It is assumed that the integral of $a \cdot n$ on Γ^- is equal to the integral of b on Γ^+.

Calculus of variations is done in H_0, the space of square integrable divergence free functions in Ω.

$$\delta J = \int_{D \times (0,T)} (u - u_d) \delta u; \quad \int_{\Omega \times (0,T)} v(\partial_t \delta u + \nabla \cdot (\delta u \otimes u + u \otimes \delta u)) = 0 \tag{8}$$

for all $v \in H_0$; $a \otimes b$ is the tensor $a_i b_j$ and below we will use the notation $A : B = \sum_{ij} A_{ij} B_{ij}$. Let $u^* \in H_0^*$ be solution of

$$\partial_t u^* + u \cdot \nabla u^* - (\nabla u) u^* + \nabla p^* = 1_D (u - u_d), \; \nabla \cdot u^* = 0, \; u^*|_{t=T} = 0 \tag{9}$$

with $u^* = 0$ on Γ^+, and $u^* \cdot n = 0$ on $\Gamma^0 \cup \Gamma^-$.

Notice that $\nabla(u^* \cdot u) = (\nabla u^*)u + (\nabla u)u^*$; so by integrating (9) multiplied by δu and performing an integration by parts :

$$\delta J = \int_{\Omega \times (0,T)} \delta u \cdot (\partial_t u^* + u \cdot \nabla u^* + (\nabla u^*)u + \nabla(p^* - u^* \cdot u))$$
$$= -\int_{\Omega \times (0,T)} (u^* \cdot \partial_t \delta u + \nabla \delta u : u \otimes u^* + u^* \nabla \cdot (\delta u \otimes u))$$
$$+ \int_{\Gamma \times (0,T)} \delta u \cdot (n \cdot u \ u^* + n \cdot u^* \ u + (p^* - u^* \cdot u)n) \tag{10}$$

The middle integral reduces to the integral of $-u^* \nabla \delta p$ because of (8) . Finally, as $u^* \cdot n = 0$ on Γ,

$$\delta J = \int_{\Gamma^- \times (0,T)} (a \cdot n \ u^* \cdot \delta a + (p^* - a \cdot u^*)\delta a \cdot n). \tag{11}$$

2.2   The Discrete Case

Let us use a finite element approximation for u of degree 2 on a triangulation $\mathcal{T}_h$ and of degree 1 for p. With the characteristic-Galerkin method [23] at each time step one has to solve: $\forall v_h \in V_h^2, \quad \forall q_h \in V_h^1$, with $v_h|_{\Gamma^-} = 0, v_h \cdot n|_\Gamma = 0$,

$$\int_\Omega (\frac{u_h^{m+1}}{\delta t} + \nabla p^{m+1})v_h - \int_\Omega q_h \nabla \cdot u_h^{m+1} = \int_\Omega \frac{1}{\delta t} u_h^m (x - \delta t u_h^m(x))v_h(x)\mathrm{d}x$$
$$\text{with } V_h = \{w_h \in C^0(\Omega_h) \ : \ w_h|_T \in P^1(T_k) \text{ for all triangles } T_k \in \mathcal{T}_h\} \tag{12}$$

It is not hard to prove (see Appendix A) that

$$\delta J = \delta t \sum_m \int_\Omega (u_h^{*\,m} \cdot (u_h^m \cdot \nabla \delta a_h) + \delta a_h \cdot (u_h^{*\,m} \cdot \nabla u_h^m) - p_h^{*\,m} \nabla \cdot \delta a_h) \tag{13}$$

with the adjoint state defined by

$$\int_\Omega (\frac{v_h}{\delta t} + \nabla q_h)u_h^{*\,m} - \int_\Omega p_h^{*\,m} \nabla \cdot v_h = \int_D (u_h^{m+1} - u_d)v_h$$
$$+\frac{1}{\delta t} \int_{\Omega^+} u_h^{*\,m+1}(y + \delta t u_h^{m+1}(x))v_h(y)\mathrm{d}y - \int_\Omega v_h u_h^{*\,m+1} \cdot \nabla u_h^{m+1}(y)\mathrm{d}x$$
$$u_h^*(T) = 0, \ \ u_h^*|_{\Gamma^+} = 0, \ \ u_h^* \cdot n|_\Gamma = 0. \tag{14}$$

for all v_h, q_h with $v_h|_{\Gamma^+} = 0, v_h \cdot n|_\Gamma = 0$. In view of the fact that the integral is on the boundaries triangles only and that the gradients are differences from the value of the functions on the boundary and zero on the opposite side of the triangles we see that (74) is a discretization of (11).
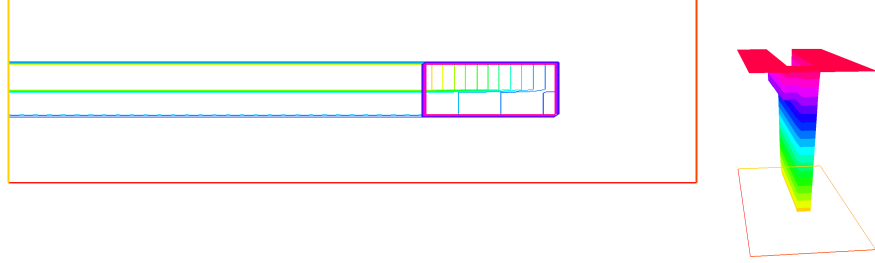
4

Figure 1: *Level lines of the adjoint equation to problem (7). In the bottom part of the channel $u = (2,0)^T$ and in the upper part $u = (1,0)^T$. The criteria involves an integral of $(u_1 - 3)^2$ in the box shown in the middle of the channel. The plot shows the horizontal component of the adjoint state in duality with u: it is discontinuous on 3 horizontal lines left of the box and in the box. The figure on the right is a front 3D view of the same.*

2.3 Contact Discontinuities: Vortex Sheet

What happens when the flow is discontinuous as in the case of contact discontinuities?

As an illustration we considered $\Omega = (0,7) \times (0,2)$ with $u(0) = [1 + 1_{y<1}, 0]^T$, $a(y) = u(0)|_{x=0}$ and other boundary conditions chosen so that $p = 0$ on the boundary, with $u_d = (3,0)^T$ and $D = (4,5) \times (0.7, 1.3)$. Although there is an obvious analytical solution (the solution is stationary : $u = u(0), p = 0$) the adjoint has been computed numerically by solving (14) with the P^2/P^1 element; the numerical test shows that the adjoint is discontinuous (fig 1). The scheme handles the situation perfectly, without oscillation.

2.4 Conclusion

From this example we see that both the continuous and the discrete problems can be derived by calculus of variations; however the computations are formal and although the discrete formulae seem to be a discretization of the continuous one it does not appear easy to prove rigorously.

Notice also that by a deriving a discrete adjoint the upwinding term for the adjoint equation is naturally in the right direction.

3 Generalization to Shocks

In the presence of shocks, several problems arise with formidable mathematical difficulties: existence and uniqueness of solution, well posedness of the adjoint equations, continuity of these with respect to boundary data, etc. But there is

one difficulty which even a mindless practitioner cannot ignore: shocks! Indeed even the formal calculation no longer makes sense in the presence of shocks.

For example if the density ρ and the velocity u are discontinuous, but with ρu continuous, it is meaningless to write

$$\delta(\rho u) = u\delta\rho + \rho\delta u \tag{15}$$

because $\delta\rho$ and δu contain Dirac singularities which cannot be multiplied by a discontinuous function if both singularities are at the same point.

Indeed let $H(x)$ be the Heaviside function (zero when $x < 0$, 1 otherwise); assume that $\rho(x)$ has a shock at $x = x_s(a)$ where a is a parameter:

$$\rho = \rho^- + (\rho^+ - \rho^-)H(x - x_s) \tag{16}$$

Assuming that not only the position of the shock x_s but also $\rho^\pm$ depends on the parameter a then by differentiation

$$\begin{aligned}
\delta\rho &= \rho^{-\prime}\delta a + (\rho^{+\prime} - \rho^{-\prime})H(x - x_s)\delta a - x_s{}'(\rho^+ - \rho^-)\underline{\delta}(x - x_s)\delta a \\
&= \rho'\delta a - x_s'[\rho]\underline{\delta}(x - x_s)\delta a
\end{aligned} \tag{17}$$

where primes denote pointwise derivatives with respect to a; this is because the derivative of H is the Dirac mass $\underline{\delta}$. So the Dirac-singularity of $\delta\rho$ is at the same point as the discontinuity of u.

3.1   Extended Calculus of Variations

Although (15) is not allowed, yet there is a way out:

$$\delta(\rho u) = (\delta\rho)\overline{u} + \overline{\rho}\delta u \tag{18}$$

where $\overline{\rho}$ (and $\overline{u}$) stands for the mean value of ρ at all points:

$$\overline{\rho}(x) = \frac{1}{2}(\rho(x^+) + \rho(x^-))$$

This idea has be used in [28, 2] to extend calculus of variation to discontinuous functions. Indeed when ρu is continuous across the shock, there is no Dirac mass on the left hand side of (18); let us show that there is no Dirac mass on the right either.

Let $[u]$ denote the jump across the shock, i.e. the value on the right side of the shock minus the value on the left side, then on the right hand side of (18) the weight of the Dirac mass is

$$\begin{aligned}
-[\rho]x_s'\delta a\overline{u} - [u]x_s'\delta a\overline{\rho} &= -x_s'\frac{\delta a}{2}((\rho^+ - \rho^-)(u^+ + u^-) + (u^+ - u^-)(\rho^+ + \rho^-)) \\
&= -x_s'\delta a[\rho u] = 0
\end{aligned} \tag{19}$$

Even if $[\rho u] \neq 0$ the weights on the Dirac masses are the same on both sides, so (18) is true pointwise and singularitywise at the shock.

More complex functions need to be decomposed into elementary products; for instance to compute the extended variation of ρ^{-1} one writes

$$1 = \frac{\rho}{\rho} \;\Rightarrow\; 0 = \frac{\overline{1}}{\rho}\delta\rho + \bar{\rho}\delta(\frac{1}{\rho}) \;\Rightarrow\; \delta(\frac{1}{\rho}) = -\frac{\overline{1}}{\rho}\frac{1}{\bar{\rho}}\delta\rho \tag{20}$$

Similarly $\rho^{-1}u^2$ being $(\rho^{-1})v$ with $v = uu$, the mean value can be computed as such. For non-rational functions $f(\rho)$ which cannot be decomposed into elementary products (like $\sin\rho$), the overline operator on derivatives is the Volpert ratio:

Definition

$$\overline{f'(\rho)} := \begin{bmatrix} \frac{[f(\rho)]}{[\rho]} & \text{at shocks,} \\ f'(\rho) & \text{at regular points} \end{bmatrix} \tag{21}$$

This is consistent with (17) :

$$
\begin{aligned}
\delta f(\rho) \;&= f'(\rho(x))\delta\rho(x) - [f]x_s'\underline{\delta}(x - x_s) \;&= f'(\rho)\delta\rho|_{x\neq x_s} - \frac{[f]}{[\rho]}[\rho]x_s'\underline{\delta}(x - x_s) \\
&= f'(\rho)\delta\rho|_{x\neq x_s} + \overline{f'(\rho)}\delta\rho|_{x=x_s} \;&= \overline{f'(\rho)}\delta\rho
\end{aligned}
\tag{22}
$$

For vector or matrix valued functions one should use the identity

$$[F(u)] = \int_0^1 F_u'(su^+ + (1 - s)u^-)\mathrm{d}s \tag{23}$$

and the Volpert ratio on each component.

4 Shocks and the Adjoint of Burgers' Equation

4.1 Analytical check

First consider the following example:
 Given a parameter $a \in \mathbf{R}$, consider the entropy solution of

$$\partial_t u + \partial_x(\frac{u^2}{2}) = 0 \quad u(x,0) = (1 + a)(1 - H(x)) \tag{24}$$

The solution is explicit and its derivative with respect to a can be computed analytically

$$
\begin{aligned}
u &= (1 + a)(1 - H(x - \frac{1+a}{2}t)), \\
u_a' &= 1 - H(x - \frac{1+a}{2}t) + \frac{1+a}{2}t\underline{\delta}(x - \frac{1+a}{2}t)
\end{aligned}
\tag{25}
$$

Let

$$J(a) := \frac{1}{2}\int_{-\frac{1}{2}}^{\frac{1}{2}} u(T)^2 = \frac{1}{4}(1+a)^2((1+a)T - 1) \tag{26}$$

Then $J'(0) = \frac{1}{4}(3T - 2)$.

To recover this by the extended calculus of variation, one proceeds as follows:

$$J' = \int_{-\frac{1}{2}}^{\frac{1}{2}} \bar{u}u'_a|_T = \int_{-\frac{1}{2}}^{\frac{1}{2}} \bar{u}^* u'_a|_0 = \int_{-\frac{1}{2}}^{0} u^*(x,0) \tag{27}$$

with u'_a solution of

$$\partial_t u'_a + \partial_x(\bar{u}u'_a) = 0, \quad u'_a(0) = 1 - H(x)$$

and u^* defined by

$$\partial_t u^* + \bar{u}\partial_x u^* = 0, \; u^*|_T = \overline{J'_u} = \bar{u}|_T \mathbf{1}_{[-\frac{1}{2}, \frac{1}{2}]} \tag{28}$$

Therefore

$$u^*(x,0) = 1 - \frac{1}{2}H(x + \frac{T}{2}) - \frac{1}{2}H(x - \frac{T}{2}) \tag{29}$$

and (27) and (26) agree.

Notice that u^* is integrated backward in time; it is constant on the characteristics, lines of slope $1 + a$ on the left of the shock and of slope 0 on the right. So the characteristics do not define u^* everywhere: there is a "shadow" triangle where no upgoing characteristics cross the line $t = T$. However thanks to the overline on u in (28) there is one characteristic of slope $\frac{1}{2}(1+a)$ on which $u^* = \bar{u}(T)$, the shock line in fact. Once u^* known on the shock line then any point in the shadow triangle has an upgoing characteristic which crosses the shock and so u^* is also known there, constant in this example and equal to $\bar{u}(T)$.

Notice that u^* is continuous across the shock and discontinuous at the characteristics that meet the shock at $t = T$.

4.2 Numerical check

Whether a numerical scheme will be capable of such a reconstruction is a matter of wonder.

Consider another example with $T = 2$ for which one seeks to compute the sensitivity with respect to a at $a = 0$:

$$J(a) = \frac{1}{2}\int_{\mathbf{R}^+} |u(x,T)|^2 \mathrm{d}x \; : \; \partial_t u + \partial_x \frac{u^2}{2} = 0, \; u|_0 = -\min(\mathrm{atan}(x + a), 0) \tag{30}$$

Although there is no shock at time zero, one develops later. The following conservative finite difference scheme has be used

$$\frac{u_i^{m+1} - u_i^m}{\delta t} + s_i \frac{u_i^{m2} - u_{i-1}^{m2}}{2\delta x} + (1 - s_{i+1})\frac{u_{i+1}^{m2} - u_i^{m2}}{2\delta x} = 0$$

$$\text{with } s_i = 1 \text{ if } u_i^m + u_{i-1}^m > 0, \quad 0 \text{ otherwise} \tag{31}$$

When J is approximated by $\frac{1}{2}\sum_{i:x_i>0}|u_i^M|^2$, the discrete Adjoint to (31) is,

$$\frac{u_i^{*m-1} - u_i^{*m}}{\delta t} + \frac{u_i^m}{\delta x}(u_i^{*m}s_i - u_{i+1}^{*m}s_{i+1} + u_{i-1}^{*m}(1-s_i) - u_i^{*m}(1-s_{i+1})) = 0$$
$$u_i^{*M} = u_i^M \tag{32}$$

with $s_i = s_i^+ - s_i^- = \text{sign}(u_i^m + u_{i-1}^m)$. Then

$$\delta J = -\sum_{i=1}^{N-1}(-u_i^{*0} + \frac{\delta t}{\delta x}u_i^0(u_i^{*0}s_i - u_{i+1}^{*0}s_{i+1} + u_{i-1}^{*0}(1-s_i) - u_i^{*0}(1-s_{i+1}))\delta u_i^0 \delta x$$

On this simple example the adjoint u^* seems to be correctly calculated by the conservative scheme (see Figure 2).

The results of Table 1 show that the scheme computes J correctly. Automatic differentiation of the computer program also gives the correct $J_a'(0)$. On figure 2 the solution and its derivative with respect to a are shown.

$J(0)$	$J(\delta a)$	$(J(\delta a) - J(0))/(\delta a)$	$J_a'(0)$	$^A J_a'(0)$
0.195009	0.190057	-0.4952	-0.492863	-0.492863

Table 1: Scheme (31) gives the correct result for J and J_a'. A computation of $J_a'(0)$ has also been done by finite difference with $\delta a = 0.01$ then with the discrete gradient (32) using the discrete adjoint and finally with Automatic Differentiation : $^A J_a'(0)$.
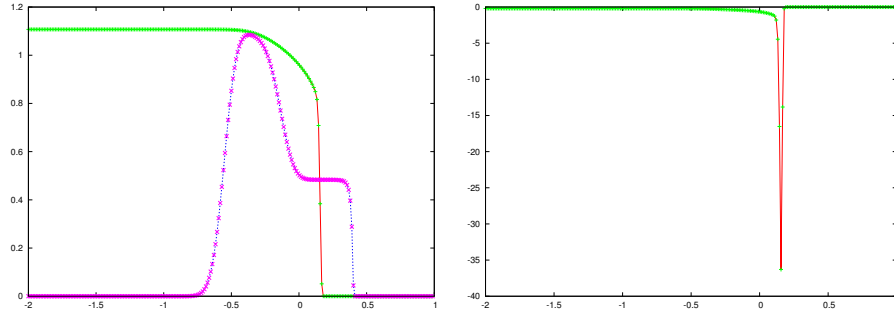

Figure 2: Left displays at T=0.325 u (green) solution of Burgers' equation and the adjoint state u^* (red), while u_a' is shown on the right. Notice the Dirac-like singularity of u_a'.

4.3 Stationary problems

The stationary case is difficult but it can be investigated as a limit case of the time dependent problem. As an example consider

$$J := \frac{1}{2T} \int_{R\times(0,T)} u^2 \;:\; \partial_t u + \partial_x(\frac{u^2}{2}) = 0 \quad u(x,0) = (1+a)(1-H(x))$$

Then

$$J' = \frac{1}{T} \int_{R\times(0,T)} \bar{u}u' \;\; \text{with } \partial_t u' + \partial_x(\bar{u}u') = 0 \quad u'(x,0) = (1-H(x))$$

The adjoint equation is

$$\partial_t u^* + \bar{u}\partial_x u^* = \frac{1}{T}\bar{u}, \; u^*|_T = 0 \tag{33}$$

and then at $a = 0$

$$J' = \int_R u'(0)u^*(0) = \int_R (1-H(x))u^*(0) = \int_{-\infty}^0 u^*(0)$$

Here too u^* is continuous at the shock.

4.4 Convergence

For scalar conservation laws in 1D the extended calculus of variation has been justified by S. Ulbrich [27]. He introduced the concept of shift derivatives for functions of bounded variations on an interval $I = [a,b]$. The idea is that if $\rho \in BV(I)$ it may have discontinuities at $a \in I$, so - as explained in (16,17) - on top of the usual variation in magnitude $\delta\rho$, the variations of the position of the discontinuities should also be considered. The result is not a function but a distribution, however a Dirac mass can be approximated by a large function on a small support, so (17) can also be written as

$$\delta\rho = \rho_a'\delta a - x_{s_a}{}'[\rho](H(x-x_s-\delta a) - H(x-x_s)) \tag{34}$$

Hence Ulbrich suggests to focus on what he calls *shift-variations* of ρ which includes at singular points $a := x_s$ of ρ

$$\delta_a\rho := \text{sign}(\delta a)[\rho(a)]^- \mathbf{1}_{(a-\delta a^-, a+\delta a^+)} \tag{35}$$

where $[\rho]^-(x) = -\min(0, \rho(x^+) - \rho(x^-))$ denotes the negative part of the jump and $\delta a^\pm$ the positive and negative part of δa. Thus a general shift-variation of ρ is

$$\tilde{\delta}\rho := \delta\rho(x) + \sum_k \delta_{a_k}\rho \tag{36}$$

10

Then $u \rightarrow y(u)$ is said to be shift-differentiable at u if there exists a linear operator y'_u and a finite set of values y'_k associated with a set of singularity points a_k such that

$$y(u + \delta u) = y(u) + y'_u(u) \cdot \delta u + \sum_k y'_k \delta_{a_k} u + o(\|\tilde{\delta} u\|) \tag{37}$$

With this definition discontinuous functions can be expanded by a Taylor formula but only for a restricted class of δu.

Furthermore when it exists the shift derivative is also the distribution derivative such as the one computed for (16) above.

Ulbrich[27] proves that entropy solutions of scalar conservation laws in 1D are shift differentiable with respect to initial data under very reasonable hypotheses; the framework gives a natural way to define an adjoint and the duality formula (3) necessary for the extended calculus of variation to hold. In an other article Ulbrich and Giles [9] have studied the convergence of the discrete adjoint to the continuous one in a simple case similar to (30).

5 Extension to the Full Euler System in 2D

Let us apply the same formalism to the two dimensional Euler equations for fluids:

$$\partial_t W + \nabla \cdot F(W) = 0 \,, W(0) = 0 \tag{38}$$

where $W = (\rho, \rho u, \rho v, \rho E)^T$ is the vector of conservative variables and the tensor F represents the convective flux: $F(W) = F_1(W) \, e_x + F_2(W) \, e_y$ with

$$F_1(W) = \begin{pmatrix} \rho u \\ \rho u^2 + p \\ \rho u v \\ (\rho E + p)u \end{pmatrix} \text{ and } F_2(W) = \begin{pmatrix} \rho v \\ \rho u v \\ \rho v^2 + p \\ (\rho E + p)v \end{pmatrix}$$

Additionally we assume that W is given at time $t = 0$, and for bounded domains Ω we add boundary conditions which we will discuss later at length and which we denote loosely by $W \in W_{ad}$.

We wish to measure the change δJ of a functional J when something changes in the data (parameters) of the above problem.

For the silent business jet problem the functional is an integral of the pressure on a part S of the boundary of the domain (the ground); for the control of the outflow of a scramjet J is an integral of the density on the outflow boundary. In both cases there exists a linear map $W \rightarrow B(W) \in \mathbb{R}^d$ and a vector $b \in \mathbb{R}^d$ such that

$$J = \frac{1}{2} \int_{S \times (0,T)} |B(W) - b|^2 \tag{39}$$

The parameter (denoted by a in the previous section) could be in the shape of the business jet or of the scramjet but at this level it is not important. The extended calculus of variation on J gives :

$$\delta J = \int_{S \times (0,T)} \overline{(B(W) - b)B'} \delta W, \tag{40}$$

Turning to δW we know from above that it satisfies

$$\partial_t \delta W + \nabla \cdot (\overline{F'(W)} \delta W) = 0 , \delta W(0) = 0, \quad \delta W - \underline{A} \delta a \in W_0 \tag{41}$$

where W_0 is the tangent space to W_{ad} at W and $\underline{A} \delta a$ is the (possible) change of boundary condition du to the change $a \to a + \delta a$. So let us introduce the adjoint equation

$$\partial_t W^* + \overline{F'(W)}^T \nabla W^* = 0, \quad W^*(T) = 0. \tag{42}$$

with boundary conditionsto be chosen later. In variational form (42) is

$$\int_{\Omega \times (0,T)} (\partial_t V \cdot W^* - \overline{F'(W)}^T \nabla W^* \cdot V) + \int_\Omega W^*(0) \cdot V(0) = 0 \quad \forall V. \tag{43}$$

Let us choose $V = \delta W$, integrate by parts and use (41):

$$0 = \int_{\Omega \times (0,T)} (\partial_t \delta W \cdot W^* - \overline{F'(W)}^T \nabla W^* \cdot \delta W)$$
$$= \int_{\Omega \times (0,T)} W^* \cdot (\partial_t \delta W + \nabla \cdot (\overline{F'(W)} \delta W)) - \int_{\partial \Omega \times (0,T)} W^* \cdot (n \cdot (\overline{F'(W)} \delta W))$$

Hence

$$\int_{\partial \Omega \times (0,T)} W^* \cdot (n \cdot (\overline{F'(W)} \delta W)) = 0 \tag{44}$$

This gives a method to evaluate δJ but for each case the boundary conditions for W^* are different because they must be chosen so that δJ appears in (44) .

5.1 An example: the scramjet

Consider a scramjet (see figure 4) with supersonic flow at the inlet and the outlet on which we observe the density at the outlet S and aim at tuning the parameters so that it be constant.

When the flow is stationary and J is the integral on $S \times (0,T)$ of $(\rho/\rho_\infty - 1)^2/(2T)$ then, asymptotically in T, $B = (1,0,0,0)/\rho_\infty^2$ and $b = 1$.

When the flow is hypersonic there is no condition on W at the outflow boundary S, therefore W_{ad} is the whole space. Let W^* on S be such that

$$W^{*T} n \cdot (\overline{F'(W)}) = \overline{(BW - b)B} \text{ on } S \tag{45}$$

With $q^2 = u^2 + v^2$, S being parallel to the y-axis, this spells out as

$$W^{*T} \begin{pmatrix} 0 & 1 & 0 & 0 \\ \dfrac{(\gamma-1)}{2}q^2 - u^2 & (3-\gamma)u & (1-\gamma)v & (\gamma-1) \\ -vu & v & u & 0 \\ ((\gamma-1)q^2 - \gamma E)\,u & \left(\dfrac{p}{\rho} + E\right) - (\gamma-1)u^2 & (1-\gamma)vu & \gamma u \end{pmatrix}$$
$$= \frac{1}{\rho_\infty}(\frac{\bar\rho}{\rho_\infty} - 1)\,(1 \quad 0 \quad 0 \quad 0) \tag{46}$$

It is a non singular linear system for W^* on S solvable as

$$W_4^* = \frac{\dfrac{1}{\rho_\infty}(\dfrac{\bar\rho}{\rho_\infty} - 1)}{\left(\dfrac{\gamma-2}{2}\bar{q}^2 + \dfrac{\gamma}{\gamma-1}\bar{u}^2 + \bar{v}^2 - \gamma\overline{E}\right)\bar{u}} \tag{47}$$

$$W_3^* = -\bar{v}\,W_4^* \tag{48}$$

$$W_2^* = -\frac{\gamma}{\gamma-1}\bar{u}\,W_4^* \tag{49}$$

$$W_1^* = \left(\frac{\gamma+1}{\gamma-1}\bar{u}^2 + \bar{v}^2 - \frac{\bar{p}}{\bar\rho} - \overline{E}\right)W_4^* \tag{50}$$

6   Numerical Flow Solvers

In this section we wish to Implement numerically (47)-(50), and compare with the conditions given by Automatic Differentiation of the Euler solver.

6.1   Euler Flow Solvers

The proposed method is a vertex-centered finite volume scheme applied to simplicial unstructured meshes which uses a particular edge-based formulation with upwind elements [1, 5]. The vertex-centered finite volume formulation consists in associating with each vertex P_i of the mesh a finite volume cell, denoted C_i, which is built by joining each vertex to the middle point of its opposite edge. The common boundary between two neighboring cells C_i and C_j is called $\partial C_{ij} = \partial C_i \cap \partial C_j$. An illustration of this construction in two dimensions is shown in Figure 3.

   The finite volume method assumes W piecewise constant on the cells and integrates (38) on each cell C_i:

$$|C_i|\frac{dW_i}{dt} + \int_{\partial C_i} F(W_i) \cdot \mathbf{n}_i\, d\gamma = |C_i|\frac{dW_i}{dt} + \sum_{P_j \in \mathcal{V}(P_i)} F|_{ij} \cdot \int_{\partial C_{ij}} \mathbf{n}_i\, d\gamma = 0\,, \tag{51}$$

where $\mathbf{n}_i$ is the outer normal to cell C_i, $\mathcal{V}(P_i)$ is the set of all neighboring vertices of P_i and $F|_{ij}$ represents the constant value of $F(W)$ at interface ∂C_{ij} from the

P_i-side. The flow is calculated with a numerical flux function, denoted Φ_{ij}:

$$\Phi_{ij} := \Phi_{ij}(W_i, W_j, \mathbf{n}_{ij}) = F|_{ij} \cdot \int_{\partial C_{ij}} \mathbf{n}_i \, d\gamma \,, \tag{52}$$

where $\mathbf{n}_{ij} = \int_{\partial C_{ij}} \mathbf{n}_i \, d\gamma$. Several upwind numerical flux functions are available and can be formally written:

$$\Phi_{ij}(W_i, W_j, \mathbf{n}_{ij}) = \frac{F(W_i) + F(W_j)}{2} \cdot \mathbf{n}_{ij} + d\left(W_i, W_j, \mathbf{n}_{ij}\right) \,, \tag{53}$$

where the function $d\left(W_i, W_j, \mathbf{n}_{ij}\right)$ contains the upwind terms and depends on the chosen scheme. Here the Roe approximate Riemann solver described in [24] is used.

Roe's approximate Riemann solver is based on the Jacobian $F'(W)$:

$$\Phi^{Roe}(W_i, W_j, \mathbf{n}_{ij}) = \frac{F(W_i) + F(W_j)}{2} \cdot \mathbf{n}_{ij} + |\tilde{A}(W_i, W_j)| \frac{W_i - W_j}{2} \tag{54}$$

where $\tilde{A} = F'(\tilde{W})$ evaluated for the Roe average variables $\tilde{W} := (\tilde{\rho}, \tilde{\rho}u, \tilde{\rho}v, \tilde{\rho}E)$ as explained in [24]. For a diagonalizable matrix $A = P\Lambda P^{-1}$, $|A|$ stands for $|A| = P|\Lambda|P^{-1}$. The eigenvalues of $F'(W)$ are real and equal to u, $u + c$ and $u - c$.

Higher-order Finite Volume Methods. The previous formulation gives at best only a first-order scheme, higher-order extensions are possible with a MUSCL addition. The idea is to use extrapolated values W_{ij} and W_{ji} of W at
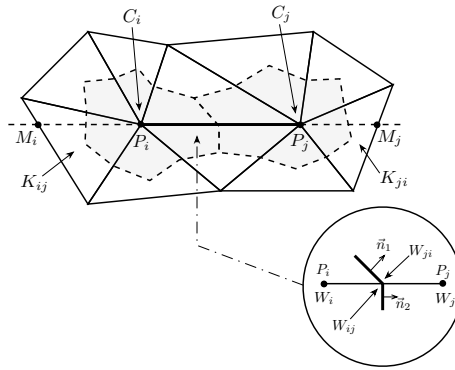

Figure 3: *Two finite volume cells C_i and C_j, and the upwind triangles K_{ij} and K_{ji} associated with edge P_iP_j. The common boundary ∂C_{ij} with the representation of the solution extrapolated for the MUSCL correction is shown.*

14

the interface ∂C_{ij} to evaluate the flux, cf. Figure 3. The following approximation is performed:

$$\Phi_{ij} = \Phi_{ij}(W_{ij}, W_{ji}, \mathbf{n}_{ij}),$$

with W_{ij} and W_{ji} which are linearly extrapolated by:

$$W_{kl} = W_k + \frac{1}{2}(\nabla W)_{kl} \cdot \overrightarrow{P_k P_l} \quad \text{with } kl = ij \, or \, ji, \tag{55}$$

where the approximate "slopes" $(\nabla W)_{ij}$ and $(\nabla W)_{ji}$ are defined on the edges by using a combination of centered, upwind and nodal gradients [1].

Such MUSCL schemes are not monotone. Therefore, limiting functions must be coupled with the previous high-order gradient evaluations to make sure that the scheme is TVD. Then ∇W_{kl} in (55) is substituted by a limited gradient denoted $(\nabla W)_{ij}^{lim}$. In this work we have used the three-entries limiter introduced by Dervieux which is a generalization of the Superbee limiter [4].

Boundary conditions. *Slip boundary conditions* are imposed for the walls because the flow is inviscid: $\mathbf{U}.\mathbf{n} = 0$. This boundary condition is imposed weakly by setting:

$$\Phi^{Slip}(W_i) = (0, p_i \, \mathbf{n}_i, 0)^t. \tag{56}$$

For free-stream external flow conditions at inflow boundaries Γ_∞ which approximate infinity, a free-stream uniform flow W_∞ is known. There, the Roe flux is replaced by the Steger-Warming flux [26]:

$$\Phi^\infty(W_i) = A^+(W_i, \mathbf{n}_i)W_i + A^-(W_i, \mathbf{n}_i)W_\infty, \tag{57}$$

where $A^\pm = \frac{1}{2}(|A| \pm A)$ and $A = F'(W)$.

At free-stream outflow boundaries no condition is imposed so nothing is done to the finite volume scheme.

Time discretization. Once the equations have been discretized in space, a set of ordinary differential equations in time is obtained: $W_t - L(W) = 0$. To discretize in time, a high-order multi-step Runge-Kutta scheme is considered. Such time discretization methods, called SSP (Strong-Stability-Preserving), have non-linear stability properties which are particularly suitable for the integration of system of hyperbolic conservation laws where discontinuities appear. The optimal 2-stage order-2 SSP Runge-Kutta scheme introduced by Shu and Osher [25] is used in this study:

$$\begin{aligned} W^{(1)} &= W^n + \delta t \, L(W^n), \\ W^{n+1} &= \frac{1}{2}W^n + \frac{1}{2}W^{(1)} + \frac{1}{2}\delta t \, L(W^{(1)}), \end{aligned}$$

The scheme is stable with a CFL coefficient close to 1. Alternatively for (38) an implicit time scheme can be used, such as Implicit Euler:

$$|C_i|\frac{W_i^{n+1} - W_i^n}{\delta t_i^n} + \Psi_i^2 W^{n+1} = 0, \tag{58}$$

where $\Psi_i^2(W^n)$ is the second order numerical flux associated with cell C_i given by the sum of the volume fluxes (53) and boundary fluxes.

7   The Numerical Scheme for the Adjoint

The adjoint of the discrete system is easier to establish when (58) is used. The linearized version of (58) is

$$\left(\frac{|C_i|}{\delta t_i^n} I_d + \Psi_i^{2'}(W^n)\right) \left(W_i^{n+1} - W_i^n\right) = -\Psi_i^2(W^n).$$

As the second order flux is too difficult to differentiate by hand, the second order Jacobian matrix is approximated by the first order one leading to:

$$\left(\frac{|C_i|}{\delta t_i^n} I_d + \Psi_i^{1'}(W^n)\right) \left(W_i^{n+1} - W_i^n\right) = -\Psi_i^2(W^n)$$

Thus the variation of the state variables δW is given by

$$\mathcal{A}^n \, \delta W^{n+1} = -\Psi^2(W^n).$$

Consequently, following Section 1.1, for Problem (38), for a given functional $J(W)$, the adjoint state W^* is defined by

$$\mathcal{A}^{n*} \, W^* = J'(W) \tag{59}$$

where $\mathcal{A}^{n*}$ is the transposed of matrix $\mathcal{A}^n$. Note however that it suffices to take $\mathcal{A}^{n*} = (\Psi_i^{1'}(W^n))^T$ because at convergence the solution does not depend on time and $\Psi_2(W^n)$ tends to 0.

7.1   Automatic differentiation of the numerical flux

Tapenade [13] is a software which takes fortran or C programs as input and returns the differentiated programs; it is done by copy-paste of the program on the web page of the Tapenade internet site. One must specify the variable(s) with respect to which the differentiation is done. It works in direct or reverse mode and the later is very similar to the adjoint method. However the result may not be optimal. For instance if a program to compute the solution of $F(u, a) = 0$ uses an iterative scheme like Newton's the differentiated code produced by Tapenade will also use Newton's method to compute u_a' such that $F_a'(u, a) + F_u'(u, a)u_a' = 0$ even though this is a linear system which can be solved directly.

In this study everything was differentiated by hand except the C-function which implements the numerical flux function which was passed to Tapenade for differentiation in direct mode. This way the full flux functions with MUSCL correction and slope limiter were differentiated. Alternatively we also wrote a solver where only a portion of the flux function is differentiated as explained below. Although full differentiation is safer, as we shall see, numerical test showed no difference when incomplete differentiation is used.

16

7.2 Manual approximate differentiation of the numerical fluxes

One reason to prefer differentiation by hand of the flux functions of the finite volume method is complete control over the source code but also execution speed.

Differentiation of Roe's flux In the Roe flux presented in Section 6 and given by (54) the Roe matrix (i.e., the dissipative matrix) is not differentiated:

$$\Phi'_{W_i}{}^{Roe}(W_i, W_j, \mathbf{n_{ij}}) \approx \frac{1}{2}\left(F'(W_i) \cdot \mathbf{n_{ij}} + |\tilde{A}(W_i, W_j)|\right)$$
$$= \frac{1}{2}\left(A(W_i) + |\tilde{A}(W_i, W_j)|\right),$$

and similarly for $\Phi'_{W_j}{}^{Roe}(W_i, W_j, \mathbf{n_{ij}})$. The analytic expression of $A(W)$ is given in Appendix B.

7.3 Differentiation of the boundary conditions.

In order to differentiate the boundary conditions, we linearize the integrals which involve a boundary flux. Indeed, a Dirichlet condition does not require any computation as it fixes some state variable at a given value.

The flux associated with the slip boundary condition is given by (56), hence using (76) in Appendix B, the following Jacobian is obtained:

$$\mathcal{A}_i^{Slip} = (\gamma - 1) \begin{pmatrix} 0 & 0 & 0 & 0 \\ \frac{q^2}{2}n_x & -un_x & -vn_x & n_x \\ \frac{q^2}{2}n_y & -un_y & -vn_y & n_y \\ 0 & 0 & 0 & 0 \end{pmatrix} \quad \text{where} \quad q^2 = u^2 + v^2.$$

For the Steger and Warming type boundary conditions, where the flux is given by (57), the linearization is direct:

$$\mathcal{A}_i^\infty = A^+(W_i, \mathbf{n}_i).$$

8 Numerical Results for a Scramjet with Outflow Control

A scramjet with supersonic flow at the inlet and the outlet has been computed with the flow solver described previously. The discrete adjoint (59) was generated by hand using exact differentiated flux generated by Tapenade or manually using (60).

When the flow is stationary and J is the integral on $S \times (0, T)$ of $(\rho/\rho_\infty - 1)^2/(2T)$ where S is the outflow boundary (parallel to the y axis), then we have

shown analytically that the boundary conditions at the outflow for the adjoint W^* are given by (47).

8.1 Numerical Results

The flow and the adjoint are shown on figure 4

The flow contains many shocks and some contact discontinuity. These emanate from the rear tip of nozzle and the adjoint density is clearly discontinuous there. By contrast it is not discontinuous at the shock lines of the density.

However shocks at the outflow boundary create discontinuous boundary conditions for the adjoints which, by analogy with Burgers' case, will propagate as discontinuities from right to left in the adjoint. The discontinuities are not on the flow shocks but around them on the characteristics which ends at the intersection of the shocks and the outflow boundary as in the one dimensional example of section 4.

Boundary Conditions on the Outflow Boundary for the adjoint   When the adjoint is generated automatically by A.D and hand transposition of the discrete equations we lose control over the boundary conditions at the outflow boundary, because are generated automatically and implement in weak form in the finite volume code.

On figure 5 the analytical values (47) are compared with the values generated by hand differentiation of the discrete solver. They agree quite well and there was no noticeable difference when the full Jacobian of the flux function computed by A.D. was used instead of the first order approximation.

We noticed however that the shocks tended to be resolved better by the analytical expressions. Note also that W_3^* has a shock but no Dirac singularity in theory while the computed value seem to have a spurious Dirac singularity.

9   Optimal Wing Profile with least Sonic Boom

Consider an airfoil Σ at rest in a semi-infinite air domain Ω. Air comes in from the left boundary L at supersonic speed and exits on the right by boundary R. Let the ground S be the lower horizontal part of the boundary ; thus the boundary of the domain is $\partial\Omega = \Sigma \cup L \cup S \cup R$. The control criteria is on the pressure p:

$$J = \frac{1}{2}\int_S (p - p_0)^2, \quad \text{therefore} \quad \delta J = \int_S (\overline{p} - \overline{p_0})\delta p.$$

The aim is to find the best admissible Σ to minimize J.

9.1   Boundary Conditions

Outflow Boundary Conditions on the Adjoint on R   The flow is supersonic so the situation is essentially the same as in section 8 for the scramjet
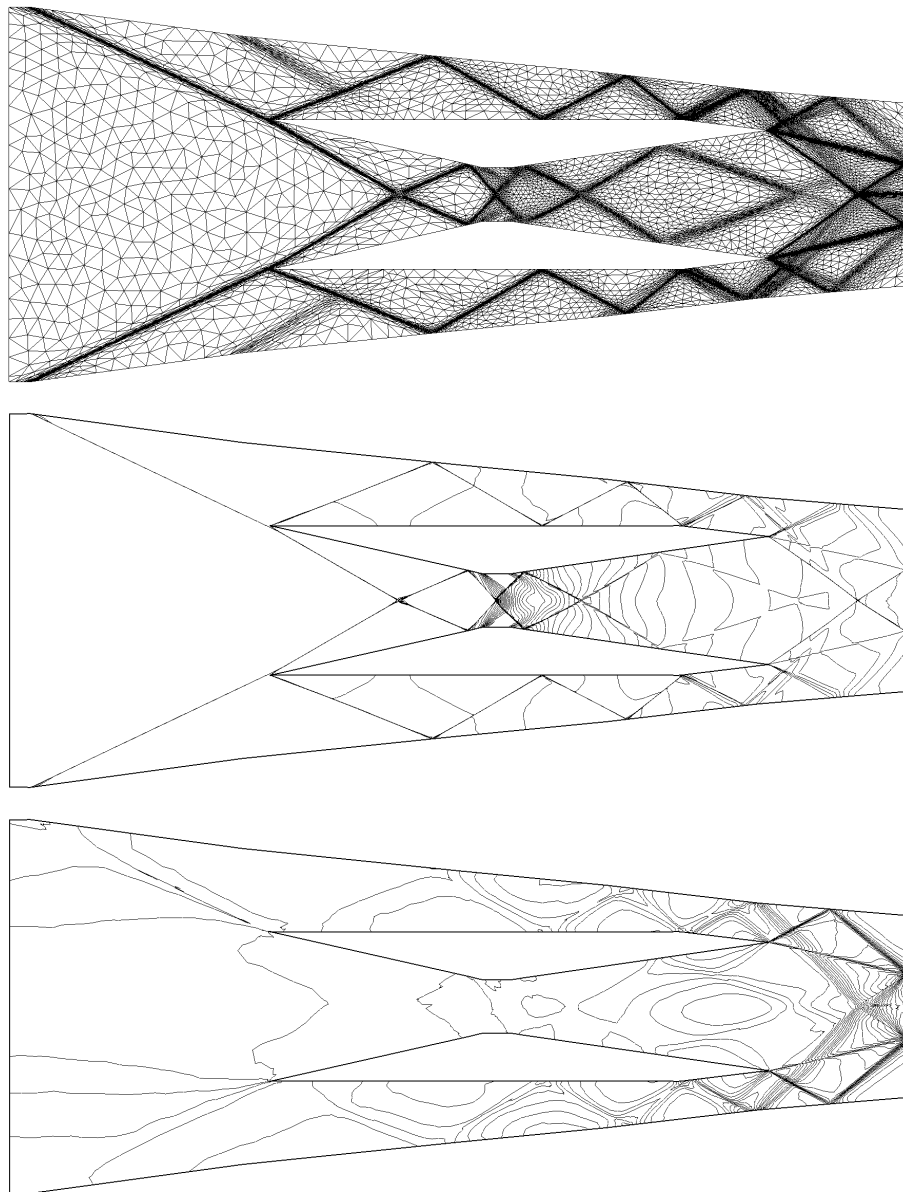
Figure 4: The scramjet: mesh (top), level lines of the density (middle) and of the adjoint density(bottom)
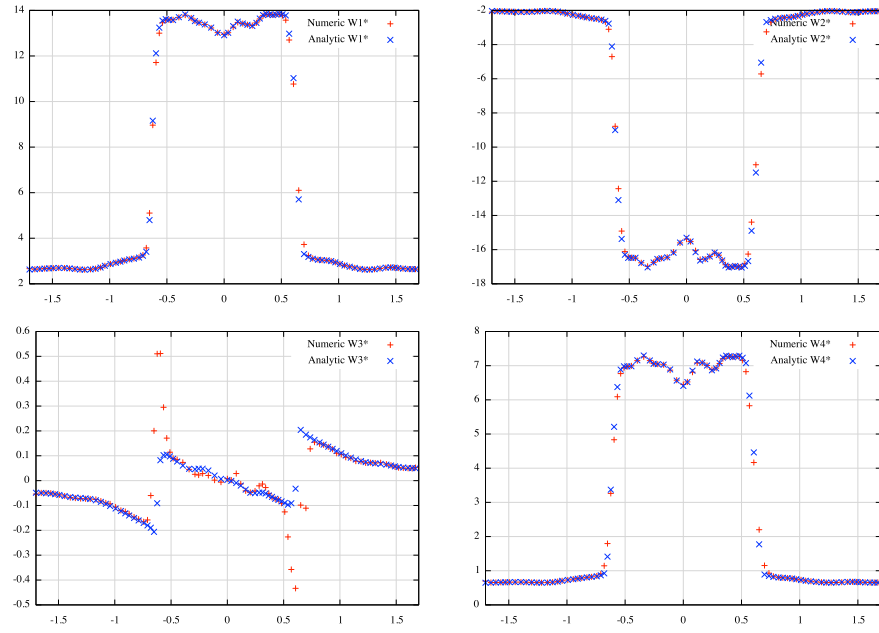
Figure 5: The scramjet, verification of (47).

except that J has no part on R so (46) has zero on the right hand side and both components of the normal n appear:

$$W^* \cdot F'(W).\vec{n} = 0$$

As $F'(W).\vec{n}$ is a non-singular matrix when the flow is hypersonic, this equation implies that all four components of W^* are zero on R:

$$W^* = 0 \text{ on } R. \tag{60}$$

Inflow Boundary Conditions for the Adjoint on L   The flow is supersonic on L so all components of the linearized flow δW are equal to zero. All the characteristics are coming in so for the adjoint state the characteristics are coming out and hence

$$W^* \text{ needs no boundary condition on } L. \tag{61}$$

Boundary Conditions for the Adjoint on the Ground S   The shock is assumed to reflect perfectly so the vertical component of the velocity is zero: $W_3 = 0$.

There is only one incoming characteristics for the linearized Euler system and for its adjoint as well. Assume that $\delta W_3 = 0$ is the boundary condition for the linearized Euler system. In [8], Giles and Pierce gave a constructive argument to choose the boundary condition for the adjoint state, in this case W_3^* should be given. Let us verify directly that it is the right choice.

On S the normal is $(0,1)^T$ and the velocity is $(u,0)^T$, so

$$n \cdot F'(W) = \begin{pmatrix} 0 & 0 & 1 & 0 \\ 0 & 0 & u & 0 \\ \dfrac{(\gamma-1)}{2}u^2 & -(\gamma-1)u & 0 & \gamma-1 \\ 0 & 0 & \gamma E - \dfrac{\gamma-1}{2}u^2 & 0 \end{pmatrix}$$

Therefore

$$W^* \cdot (n \cdot F'(W))\delta W = \begin{pmatrix} 0 & 0 & \frac{(\gamma-1)}{2}u^2\delta W_1 - (\gamma-1)u\delta W_2 + (\gamma-1)\delta W_4 & 0 \end{pmatrix} W^*$$
$$= (\gamma-1)(\frac{u^2}{2}\delta W_1 - u\delta W_2 + \delta W_4)W_3^* \tag{62}$$

On the other hand

$$p = (\gamma-1)\rho e - \frac{\gamma-1}{2}\frac{(\rho u)^2 + (\rho v)^2}{\rho} = (\gamma-1)(W_4 - \frac{W_2^2 + W_3^2}{2W_1}),$$

therefore

$$\delta p = (\gamma-1)(\frac{W_2^2}{2W_1^2}\delta W_1 - \frac{W_2}{W_1}\delta W_2 + \delta W_4) = (\gamma-1)(\frac{u^2}{2}\delta W_1 - u\delta W_2 + \delta W_4).$$

By choosing

$$W_3^*|_S = \overline{p - p_0},$$

21

(45) becomes $(p - p_0)\delta p$ and in the stationary regime (44) becomes

$$\delta J = - \int_{\partial\Omega\backslash S} W^* \cdot (n \cdot \overline{F'(W)}\delta W) \tag{63}$$

Boundary Conditions for the Adjoint on the airfoil Σ The flow is subsonic and tangent to Σ so $u \cdot n = 0$. As for S one boundary condition is required for δW. Let $\delta W \cdot n$ be given. An elementary calculus gives

$$
\begin{aligned}
W^* \cdot (F'(W) \cdot n)\delta W &= (\gamma - 1)W^* \cdot n(\frac{1}{2}(u^2 + v^2)\delta W_1 - u\delta W_2 - v\delta W_3 + \delta W_4) \\
&\quad + (W_1^* + uW_2^* + vW_3^*)\delta W \cdot n
\end{aligned}
\tag{64}
$$

As Giles and Pierce found [8] by another method, this expression contains no other δW-term but $\delta W \cdot n$ if and only if

$$W^* \cdot n = 0 \text{ on } \Sigma. \tag{65}$$

Proposition 1. *Let W^* be defined by*

$$
\begin{aligned}
&\partial_T W^* + \overline{F'(W)}^T \nabla W^* = 0, \quad W(T) = 0, \\
&W^* \cdot n = 0 \ on \ \Sigma \\
&W^*|_R = 0, \quad W_3^*|_S = \overline{p - p_0}
\end{aligned}
\tag{66}
$$

Then, asymptotically in time,

$$\delta J = - \int_\Sigma (W_1^* + \vec{U} \cdot \vec{W}_{2.3}^*)\delta\vec{W}_{2.3} \cdot \vec{n} \tag{67}$$

where $W_{2.3}$ is the vector $(W_2, W_3)^T$.

Formula (67) is essential to set up descent algorithms for optimal shape design to minimize J. The proof of the proposition is a consequence of (44),(61)(63),(65). We have assumed that there was no shock on Σ; if it is not so, mean values have to be used for the integrand in (67).

Remark 1. *It may be more readable to rewrite (67) in terms of the components of the adjoint state $(\rho^*, (\rho U)^*, (\rho e)^*)$:*

$$\delta J = - \int_\Sigma (\rho^* + \vec{U} \cdot (\rho\vec{U})^*)\delta(\rho\vec{U}) \cdot \vec{n} \tag{68}$$

9.2   A Gradient Method for Shape Optimization

Thanks to (68) we have now a method to modify the shape of the airfoil Σ to decrease J.

Following [22, 20], consider a variation Σ_α of Σ defined by the normal displacement α and given by

$$\Sigma_\alpha = \{x + \alpha(x)n(x) \ : \ x \in \Sigma\}$$

Denote W_α the new flow variables and to simplify notations introduce $V := \rho U$
By definition we have

$$V(x) \cdot n(x) = 0, \quad V_\alpha(x + \alpha n(x)) \cdot n_{\Sigma_\alpha}(x + \alpha n(x)) = 0, \quad \forall x \in \Sigma$$

Assuming differentiability and ignoring higher order terms, the second equation implies

$$0 = V_\alpha(x) \cdot n(x) + \alpha \left(\ (\nabla V(x) \cdot n(x)) \cdot n(x) + V(x) \cdot n'(x) \ \right) \qquad (69)$$

where n' is the derivative with respect to $\alpha(x)$ of n_{Σ_α}. The above is also

$$\delta V \cdot n|_\Sigma = V_\alpha(x) \cdot n(x) = -\alpha(\frac{\partial V_n}{\partial n} - \kappa V_t)$$

where t is the tangent vector associated with n – i.e. n rotated clockwise by 90 degrees – because $n' = -\kappa t$ where κ is the curvature (inverse of the radius of curvature).

Thus (see (68)) by choosing

$$\alpha = -\lambda(\rho^* + \vec{U} \cdot (\rho\vec{U})^*)(\frac{\partial(\rho U_n)}{\partial n} - \kappa\rho U_t)$$

for a small enough constant scalar λ, J will decrease because, in this case

$$\delta J = -\lambda \int_\Sigma (\rho^* + \vec{U} \cdot (\rho\vec{U})^*)^2 (\frac{\partial(\rho U_n)}{\partial n} - \kappa\rho U_t)^2 + o(\lambda)$$

This method was used by B. Mohammadi in [20] and G. Rogé et al in [6] to reduce the sonic boom of a business jet by 30% without affecting the lift. Automatic differentiation was used, so we intend to reproduce the results with the code presented here in the future. Meanwhile, as for the scramjet, let us verify that the discrete adjoint converges to the continuous one.

9.3   Numerical Tests

A supersonic flow at Mach 2 is computed around a NACA0012 airfoil flying over ground at very low altitude. (see figure 6). Euler flow and its discrete adjoint are computed on a flow-adapted mesh in 2D. The value of the adjoint on the ground S is compared with its analytical value.

Results shown on figure 7 confirm that the discrete adjoint converges to the continuous one and that it is continuous at the shocks.

Analysis of Figure 6   Here too we observe that the adjoint density is continuous at the shocks of ρ except near the ground. There the boundary condition on the adjoint forces a discontinuity which, by analogy with Burgers', should spread into shocks on the characteristics at the shock point. Since there is only one incoming characteristic we expect to have only one shock in the adjoint (while there was 2 in the case of Burgers'). On the reflected shock near the ground, the adjoint has a bump type variation. It is not clear whether it is physical or numerical. The adjoint also varies greatly near the NACA profile. A zoom shows that these variations are not discontinuities.
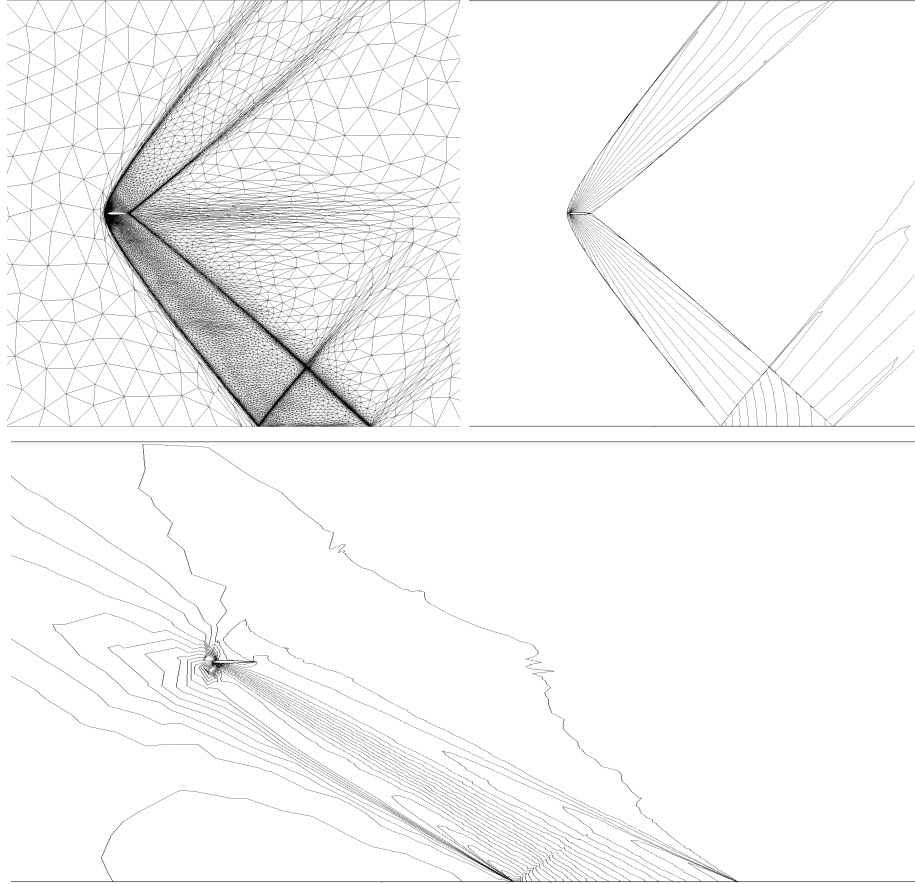
Figure 6: The NACA airfoil: the adapted mesh (top left),; the level lines of the density (top right) and (bottom, the figure is stretched horizontally) the level lines of the first component of the adjoint, i.e. the adjoint density.
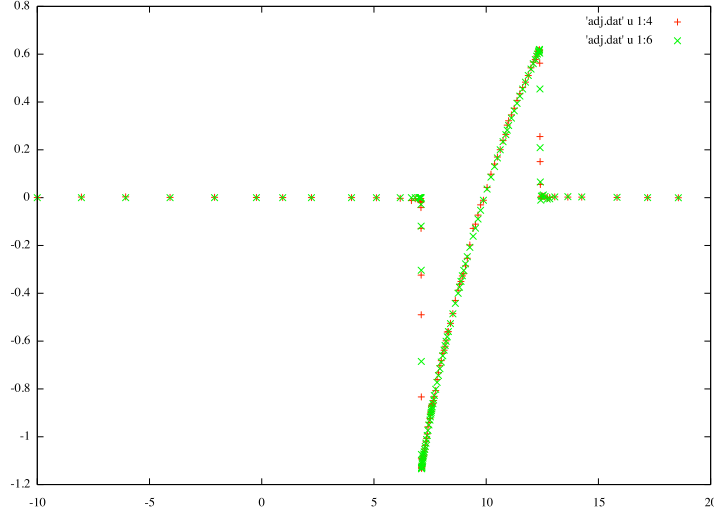
Figure 7: The NACA airfoil: comparison between W_3^*, the component of the adjoint in duality with ρv and $p - p_0$ on S. Although the adjoint's equation is generated by automatic differentiation for the discrete case, it agrees with the continuous limit (see (66))

Discrete versus Continuous Adjoint (Figure 7)   For the minimizing of the sonic boom we have seen that the theory predicts that the boundary condition of the third component of the adjoint W_3^* is $p - p_0$. On Figure 7 both quantities are displayed; the concordance is excellent. This is another indication that the adjoint obtained by automatic differentiation in reverse mode of the discrete solver converges to the continuous adjoint when the mesh is refined.

Conclusion

Industry is never happy to include an unreadable portion of code in their numerical tools; this is one reason to avoid using automatic differentiation to generate the adjoint of the Euler linearize system. By contrast A.D. is very practical and avoids code errors but theory doe not support yet the convergence when the mesh size decreases.

On the whole this numerical study validates both the automatic generation of adjoints and the hand derivation with incomplete derivatives for the flux functions (i.e. without differentiation of the MUSCL and slope limiters). It is also reassuring to see on two examples that the discrete adjoints seem to converge to the continuous adjoints.

One difficulty remains unanswered: whether the automatically generated adjoints are correct in the case of discontinuous boundary data. The theory

25

requires a precise boundary condition at the shock which the discrete adjoints don't seem to observe and even if they did a rather fine mesh would be needed to implement the condition anyway. However on the scramjet and on the airfoil this difficult did not show up in the numerical tests.

References

[1] F. Alauzet and A. Loseille: High Order Sonic Boom Modeling by Adaptive Methods. Journal of Computational Physics, Vol. 229, pp. 561-593, 2010.

[2] C. Bardos and O.Pironneau: Sensitivities for Euler Flows. C. R. Acad. Sci., Paris, Ser I 335 (2002) 839-845 (2002)

[3] R. Becker and R. Rannacher. An optimal control approach to error control and mesh adaptation. In A. Iserles, editor, Acta Numerica 2001. Cambridge University Press, 2001.

[4] P.-H. Cournède and B. Koobus and A. Dervieux, Positivity statements for a Mixed-Element-Volume scheme on fixed and moving grids, European Journal of Computational Mechanics, vol 15 (7-8):767-798, 2006.

[5] C. Debiez and A. Dervieux, Mixed-Element-Volume MUSCL methods with weak viscosity for steady and unsteady flow calculations, Comput. & Fluids, vol 29:89-118, 2000.

[6] Q.Dinh, G.Rogé, C.Sevinand and B.Stoufflet: Shape optimization in computational fluid dynamics. European Journal of Finite Elements, vol. 5, p. 569-594, 1996.

[7] M.B. Giles: Discrete adjoint approximations with shocks. In T. Hou and E. Tadmor, editors, Hyperbolic Problems: Theory, Numerics, Ap- plications. Springer-Verlag, 2003.

[8] M. Giles and N. Pierce: Adjoint Equations in CFD. AIAA 97-1850. See also: On the properties of solutions of the adjoint Euler equations. In M. Baines, editor, Numerical Methods for Fluid Dynamics VI. ICFD, June 1998.

[9] M.B. Giles and S. Ulbrich. Convergence of linearised and adjoint approximations for discontinuous solutions of conservation laws. Part 1: Linearised approximations and linearised output functionals. Technical Report, Mathematical Institute, University of Oxford, 2009.

[10] A. Griewank and D. Juedes and J. Utke: Algorithm 755: ADOL-C : a package for the automatic differentiation of algorithms written in C/ C++, j-TOMS, 22(2), 131-167. 1996.

[11] M.D. Gunzburger : Perspectives in Flow Control and Optimization. SIAM, Philadelphia. 2002.

[12] J. Hadamard: Lessons on the Calculus of Variations (in French). Gauthier-Villard. Paris 1910.

[13] L. Hascoet and V. Pascual, Tapenade 2.1 user's guide,INRIA, RT-0300, (2004). See also `www-sop.inria.fr/tropics/tapenade.htm`

[14] A. Jameson. Optimum aerodynamic design using control theory. In M. Hafez and K. Oshima, editors, Computational Fluid Dynamics Re- view 1995, pages 495?528. John Wiley & Sons, 1995.

[15] S. Kim and J.J. Alonso and A. Jameson: Design Optimization of High-Lift Configurations Using a Viscous Continuous Adjoint Method, AIAA-2002-0844, 40th AIAA Aerospace Sciences Meeting, Reno, NV, January, 2002.

[16] L. Landau and F. Lifschitz: Fluid Mechanics. Mir edition Moscow 1962.

[17] J.L. Lions. Optimal Control of Distributed Systems, Dunod 1968.

[18] A. Loseille and A. Dervieux and F. Alauzet, Fully anisotropic goal-oriented mesh adaptation for 3D steady Euler equations, J. Comp. Phys. vol 229:2866-2897, 2010.

[19] A. Loseille, F. Alauzet, A. Dervieux: Fully anisotropic goal-oriented mesh adaptation for 3D steady Euler equations. Journal of Computational Physics, Vol. 229, pp. 2866-2897, 2010.

[20] B. Mohammadi and O. Pironneau. Applied Optimal Shape Design. Oxford University Press (2nd ed.) 2009.

[21] M. Nemec and M. Aftosmis: Parallel Adjoint Framework for Aerodynamic Shape Optimization of Component-based Geometry. AIAA 2011-1249, Jan 2011.

[22] O. Pironneau. Optimal Shape Design for Elliptic Systems, Springer, Berlin. 1983.

[23] O. Pironneau: Finite Element in Fluids, John Wiley & SonsWiley, Chichester. 1983.

[24] P. Roe, Approximate Riemann solvers, parameter vectors, and difference schemes, J. Comp. Phys., vol 43:357-372, 1981.

[25] C.W. Shu and S. Osher, Efficient implementation of essentially non-oscillatory shock-capturing schemes, J. Comput. Phys., vol 77:439-471, 1988.

[26] J.L. Steger and R.F. Warming, Flux vector splitting of the inviscid gasdynamic equations with application to finite-difference methods, J. Comput. Phys., vol 40:263-293, 1981.

[27] S. Ulbrich. A sensitivity and adjoint calculus for discontinuous solu-tions of hyperbolic conservation laws with source terms. SIAM Journal of Control and Optimization, 41(3):740?797, 2002.

[28] S. Ulbrich. Adjoint-based derivative computations for the optimal con- trol of discontinuous solutions of hyperbolic conservation laws. Systems & Control Letters, 48(3-4):313-328, 2003.

10 Appendix A: Calculus of Variation for Discrete Incompressible Euler Flows

With reference to (7) and (12),

$$\delta J_h = \int_{D \times (0,T)} (u_h^{m+1} - u_d) \delta u^{m+1} \text{ with}$$

$$\int_\Omega (\frac{\delta u_h^{m+1}}{\delta t} + \nabla \delta p^{m+1}) v_h - \int_\Omega q_h \nabla \cdot \delta u_h^{m+1}$$

$$= \frac{1}{\delta t} \int_\Omega v_h(x) [\delta u_h^m(y) - \delta t \delta u_h^m(x) \cdot \nabla u_h^m(y)]|_{y=x-\delta t u_h^m(x)} dx \qquad (70)$$

Now with a change of variable $y = x - \delta t u_h^m(x)$ in the first half of the last integral, it is also

$$\frac{1}{\delta t} \int_{\Omega^+} v_h(y + \delta t u_h^m(x)) \delta u_h^m(y) dy - \int_\Omega v_h(x) \delta u_h^m(x) \cdot \nabla u_h^m(x - \delta t u_h^m(x)) dx \quad (71)$$

where $\Omega^+ = \{y := x - \delta t u_h^m(x) : x \in \Omega\}$.

The adjoint equation is obtained by replacing $\delta u_h, \delta p_h$ by v_h, q_h and v_h, q_h by u_h^*, p_h^* and adding the contribution of δJ at time $(m+1)\delta t$ on the right hand side:

$$\int_\Omega (\frac{v_h}{\delta t} + \nabla q_h) u_h^{*\,m} - \int_\Omega p_h^{*\,m} \nabla \cdot v_h = \int_D (u_h^{m+1} - u_d) v_h$$

$$+ \frac{1}{\delta t} \int_{\Omega^+} u_h^{*\,m+1}(y + \delta t u_h^{m+1}(x)) v_h(y) dy - \int_\Omega v_h u_h^{*\,m+1} \cdot \nabla u_h^{m+1}(y) dx \quad (72)$$

for all v_h, q_h with $v_h|_{\Gamma^+} = 0$, $v_h \cdot n|_\Gamma = 0$.

We choose to impose $u_h^*(T) = 0$, $u_h^*|_{\Gamma^+} = 0$, $u_h^* \cdot n|_\Gamma = 0$.

Let us replace (v_h, q_h) by $(\tilde{\delta} u_h, \delta p_h)$ where the tilde means that the value of δu_h^{m+1} at the boundary nodes of Γ^- have been put to zero to be admissible:

$$\delta J = \sum_m \delta t [\int_\Omega (\frac{\tilde{\delta} u_h^{m+1}}{\delta t} + \nabla \delta p_h^{m+1}) u_h^{*\,m} - \int_\Omega p_h^{*\,m} \nabla \cdot \tilde{\delta} u_h^{m+1}] - I \text{ with}$$

$$I = \sum_m [\int_{\Omega^+} u_h^{*\,m+1}(x) \tilde{\delta} u_h^{m+1}(y) dy - \delta t \int_\Omega \tilde{\delta} u_h^{m+1}(x) u_h^{*\,m+1}(x) \cdot \nabla u_h^{m+1}(y) dx]$$

$$= \sum_m [\int_\Omega u_h^{*\,m}(x) \tilde{\delta} u_h^m(x - \delta t u_h^m(x)) dx - \delta t \int_\Omega \tilde{\delta} u_h^m(x) u_h^{*\,m}(x) \cdot \nabla u_h^m(y) dx] \quad (73)$$

It contains the equation of $(\delta u_h, \delta p_h)$ with the test functions replaced by (u_h^*, p_h^*) it if it wasn't for the tildes. Let us call δa_h the vector value P^2 finite element function which is equal to δa at the nodes of Γ_h^- and zero at other nodes. Since $\delta u_h = \tilde{\delta} u_h + \delta a_h$ at all time steps, taking the boundary conditions into account we have up to $O(\delta t), o(\delta a_h)$ terms:

$$\delta J = \delta t \sum_m \int_\Omega (u_h^{*\,m} \cdot (u_h^m \cdot \nabla \delta a_h) + \delta a_h \cdot (u_h^{*\,m} \cdot \nabla u_h^m) - p_h^{*\,m} \nabla \cdot \delta a_h). \qquad (74)$$

29

Appendix B: Jacobian matrix in 2D

In two dimensions, the Euler equations could be symbolically rewritten:

$$\partial_t W + \nabla \cdot F(W) = 0\,, \tag{75}$$

where $W = (\rho, \rho u, \rho v, \rho E)^T$ is the conservative variables vector and the vector F represents the convective operator. The vector F may be decomposed as $F(W) = F_1(W)\, e_x + F_2(W)\, e_y$ with $p = (\gamma - 1)\rho E - \dfrac{\gamma - 1}{2}\dfrac{(\rho u)^2 + (\rho v)^2}{\rho}$ and

$$F_1(W) = \begin{pmatrix} \rho u \\ \rho u^2 + p \\ \rho uv \\ (\rho E + p)u \end{pmatrix} \quad \text{and} \quad F_2(W) = \begin{pmatrix} \rho v \\ \rho uv \\ \rho v^2 + p \\ (\rho E + p)v \end{pmatrix}$$

The Jacobian of p with respect to the conservative variable is:

$$\frac{\partial p(W)}{\partial W} = (\gamma - 1)\, {}^t\left(\frac{q^2}{2}\,, -u\,, -v\,, 1 \right) \tag{76}$$

where $q^2 = u^2 + v^2$. After simplifications, the Jacobians read:

$$\frac{\partial F_1(W)}{\partial W} = \begin{pmatrix} 0 & 1 & 0 & 0 \\ \dfrac{(\gamma - 1)}{2}q^2 - u^2 & -(\gamma - 3)u & -(\gamma - 1)v & \gamma - 1 \\ -uv & v & u & 0 \\ ((\gamma - 1)q^2 - \gamma E)u & \gamma E - \dfrac{\gamma - 1}{2}\left(2u^2 + q^2\right) & -(\gamma - 1)uv & \gamma u \end{pmatrix},$$

$$\frac{\partial F_2(W)}{\partial W} = \begin{pmatrix} 0 & 0 & 1 & 0 \\ -uv & v & u & 0 \\ \dfrac{(\gamma - 1)}{2}q^2 - v^2 & -(\gamma - 1)u & -(\gamma - 3)v & \gamma - 1 \\ ((\gamma - 1)q^2 - \gamma E)v & -(\gamma - 1)uv & \gamma E - \dfrac{\gamma - 1}{2}\left(2v^2 + q^2\right) & \gamma v \end{pmatrix},$$

For an edge $\mathbf{e}$ with $\mathbf{n}$ as normal vector, we have: $A(W) := \dfrac{\partial F(W).\mathbf{n}}{\partial W} =$

$$\begin{pmatrix} 0 & n_x & n_y & 0 \\ \dfrac{\gamma_1}{2}q^2 n_x - u\,\mathbf{u}\cdot\mathbf{n} & \mathbf{u}\cdot\mathbf{n} - (\gamma - 2)un_x & u\,n_y - (\gamma - 1)vn_x & \gamma_1 n_x \\ \dfrac{\gamma_1}{2}q^2 n_y - v\,\mathbf{u}\cdot\mathbf{n} & v\,n_x - \gamma_1 un_y & \mathbf{u}\cdot\mathbf{n} - (\gamma - 2)vn_y & \gamma_1 n_y \\ \left(\gamma_1 q^2 - \gamma E\right)\mathbf{u}\cdot\mathbf{n} & \left(\dfrac{p}{\rho} + E\right)n_x - \gamma_1 u\mathbf{u}\cdot\mathbf{n} & \left(\dfrac{p}{\rho} + E\right)n_y - \gamma_1 v\mathbf{u}\cdot\mathbf{n} & \gamma\,\mathbf{u}\cdot\mathbf{n} \end{pmatrix}$$

where $\mathbf{u} = (u, v)$, $\gamma_1 = \gamma - 1$ and $\mathbf{n} = (n_x, n_y)$.